Int. J. Electrochem. Sci., 17 **(2022)** Article Number: 220729, doi: 10.20964/2022.07.06

International Journal of
ELECTROCHEMICAL
SCIENCE
www.electrochemsci.org

A Highly Sensitive Cefotaxime Electrochemical Detection Technique Based on Graphene Quantum Dots

Mengting Duan[1,2], *Xiaowen He*[1,2], *Qiu Zhang*[1,2], *Bingxin Zheng*[1,2*]

[1] Department of Pharmacy, The First Hospital of China Medical University, No.155 Nnajing Street, Heping District, Shenyang 110000, China
[2] School of Pharmacy, China Medical University, Shenyang, Liaoning Province, 110001, China
[*]E-mail: 324334707@qq.com

Received: 7 March 2022 / *Accepted:* 20 April 2022 / *Published:* 6 June 2022

Antibacterial drugs are one of the greatest achievements in the field of medicine and play an extremely important role in improving human health. However, the human antimicrobial resistance and the harm of residues in animal food to human body have continued to be concerned. In this work, a cefotaxime electrochemical sensor was constructed based on graphene quantum dots and poly(arginine) (Parg) modified electrode. Scanning electron microscopy and Fourier transform infrared spectroscopy showed that L-arginine was polymerized on the electrode surface. The result of electrochemical impedance and cyclic voltammetry further demonstrate that graphene QDS/Parg films can effectively increase the electron transfer rate on the electrode surface, which indicates that the modified electrode can be applied to the quantitative determination of cefotaxime. In the study, the peak current on the electrode showed a good linear relationship with the concentration of cefotaxime. The linear range was 0.07-450 μM, and the minimum detection limit was 34 nM.

Keywords: Electrochemical sensor; Cephalosporins; Glassy carbon electrode; Graphene quantum dots; Electrochemical behavior

1. INTRODUCTION

In recent years, researchers have focused on the development of new antibacterial drugs. The range of antibacterial spectrum is also increased, thus the bacterial infectious diseases have been effectively controlled [1–3]. However, if antibiotics are not used in large quantities or in excess, bacteria in the body can become resistant to them, reducing their effectiveness. In addition, in animal husbandry, excessive use of antibacterial drugs will lead to excessive accumulation of drug molecules or their metabolites in animal cells or edible products. Excessive, improper and unrestricted use of antibiotics are all regarded as abuse [4,5]. Bacterial drug resistance is a biological phenomenon in which

microorganisms constantly evolve in order to survive, reproduce and resist adverse external environment [6–9]. It means that after the use of antibiotics for a period of time, the dosage must be increased, otherwise the therapeutic effect will decline or even invalid. Discontinued usage will make resistance that has developed decline, and bacteria continue to rise rapidly. Antibacterial drugs kill pathogens and in the meantime harm the human body. In addition, a number of antibacterial drugs such as penicillin can also produce allergic reactions, which damages the nervous system [10,11]. The abuse of antibacterial drugs allows the bacteria to contact with drugs repeatedly, resulting in reduced sensitivity of bacteria to drugs. It can also cause pathogenic bacteria that are not dominant to survive and multiply, being resistant to drugs [12–14].

Cephalosporin antibiotics belongs to β-lactam class of drugs, which has significant effect on fighting against gram positive bacteria and negative bacteria effect [15,16]. Due to their effective antibacterial activity and pharmacokinetic characteristics, they has been widely adopted in clinical and drug therapies [17,18]. The therapeutic mechanism for their antibacterial activity is to prevent bacterial growth by reducing their peptidoglycan. Cefotaxime is the third generation semi-synthetic cephalosporin, which is mainly used to treat various infections caused by bacterial strains susceptible to infection, such as respiratory tract infection, urogenital infection, gynecological infection, skin infection and central nervous infection [19,20].

Antibacterial drugs have huge influence on human health and life, thus the detection of antibacterial drug content is of great importance [21,22]. At present, the commonly used methods for the detection of antibacterial drugs include high performance liquid chromatography, gas chromatography, thin layer chromatography, nuclear magnetic resonance spectrometry, capillary electrophoresis, spectrophotometry, chemiluminescence and electrochemical analysis [23–26]. Each of the above methods has played a positive role in the field of drug analysis and each has its own strengths and weaknesses [7,10,27]. For example, despite that the spectral method is simple, it has a relatively lower sensitivity and poor anti-interference ability[28–30]. The main advantages of chromatography are reflected in the separation of multiple components, but the preparation and operation of chromatographic column is complicated with high cost [31–35]. Capillary electrophoresis and flow injection analysis have low capacity of sample processing and are both time-consuming. Compared with the above methods, electrochemical method has obvious advantages [36], including low cost, rapid response, high sensitivity, simple operation and large sample handling capacity [37,38]. However, shortcomings still exist and the most important one is that electrode repeatability and stability need to be improved.

Recently, researchers discovered a novel quasi - zero dimensional carbon nanomaterial graphene quantum dots (GQD), which are characterized by high electrical mobility, specific surface area, strong biological affinity, low toxicity, good water solubility and abundant surface activity. GQD have been studied in various fields including biological imaging, luminescence analysis, metal ions and organic small molecule detection, etc. [39–43]. Previously, the electrochemical sensing of H_2O_2 by graphene quantum dots has been reported. For example, Zhang et al. [44] prepared a gold electrode modified by GQD with electrostatic self-assembly technology and applied it in the detection of H_2O_2. Ju et al. [45] used nitrogen-doped GQD as reducing agent to prepare gold-GQD composite nanomaterials in situ by thermal reflux technology, and modified the electrode with this material to achieve highly sensitive determination of H_2O_2. Moreover, poly (amino acid) modified electrodes have been increasingly used

in the determination of a variety of substances, such as drugs, amino acids, etc. The polymerization of amino acids on the electrode is obtained by dehydration of —NH_2 and —COOH. L-arginine has positively charged guanidine groups that can be bound to negatively charged groups through hydrogen bonding and electrostatic interaction. Because of the special structure of arginine, poly-arginine has been applied in the detection of some small biological molecules [46–50].

In this study, a novel sensor based on GQD and polyarginine modified glassy carbon electrode (GQD/Parg/GCE) was prepared and applied to the quantitative detection of cefotaxime. The composite was characterized by spectroscopic and electron microscopy. The results show that the introduction of graphene quantum dots can improve the permeability and conductivity of the modified electrode surface. The sensor has strong catalytic activity for the electrooxidation of cefotaxime. Compared with other reported modified electrodes, this electrode has a wide linear range, low detection limit and high sensitivity in detecting cefotaxime, which is expected to be adopted for the determination of hydrogen peroxide content in actual water samples.

2. EXPERIMENTAL

Natural flake graphite (less than 30 μm, and the carbon content is 99.9%) was purchased from Nanshu Developed Graphite Company, Laixi City, Qingdao. L-arg was purchased from Shanghai Sinopharm Chemical Reagent Co., LTD. Hydrogen peroxide (30% H_2O_2) was purchased from Zhengzhou Paini Chemical Reagent Factory. Cefotaxime was purchased from Xinyag Mutong Co., LTD. All reagents are analytically pure and can be used directly in experiments without treatment.

CHI 760D Electrochemical Workstation (Shanghai Chenhua Instrument Co., LTD.) was adopted for all electrochemical investigations. A three-electrode system was applied: modified electrode working electrode, platinum wire electrode counter electrode, and saturated calomel electrode (SCE) that was used as reference electrode. Hitachi F-4500 fluorescence spectrophotometer (Hitachi Corporation of Japan) was adopted for fluorescence detection of materials, and Model 8453 UV-Visible Spectrophotometer (Agilent) for UV-VIS spectra acquisition. A ReactIR 45m spectrometer and a 1.5 m silver halide optical fiber ATR probe with a diamond tip (Mettler Toledo, Columbus, OH) were used to record FTIR spectrum. SEM images were recorded with Zeiss EVO 18 scanning electron microscope operated at an accelerating voltage of 10 kV.

First of all, GO was prepared by an improved Hummers method, after which 100 mg GO was weighed and added into 13. 00 mL water for ultrasound for 10 min, and 12. 00 mL 30% H2O2 was added to control water bath at 95 ℃, which was stirred for 17 h. The reaction was stopped when the solution changed from black to bright yellow, and then the solution was dialyzed in a 3 500 Da dialysis bag for 48 h to prepare a solution of graphene quantum dots (GQD).

Polyarginine modified GCE (Parg/GCE) was obtained by CV scanning. GCE was immersed in 0.1m B-R buffer solution containing 1.0 mm arginine and scanned for 10 cycles with cyclic voltammetry at scanning potential -2.0—2.5V and scanning speed of 100 mV/s. Afterwards, 10 μL GQD was dropped into Parg/GCE to dry naturally (GQD/Parg/GCE). The 10 mM redox couple solution ($[Fe(CN)6]^{3-/4-}$)

was prepared by dissolving potassium ferrocyanide ($K_4[Fe(CN)_6]$) and potassium ferricyanide ($K_3[Fe(CN)_6]$) in B-R buffer has been adopted for EIS measurements.

3. RESULTS AND DISCUSSION

In this study, GQD was prepared by chemical etching of GO with hydrogen peroxide being the oxidant. Figure 1A shows the fluorescence spectrum of GQD obtained. It can be noted that GO alone has almost no emission peak, while GQD has an obvious emission peak at 508 nm [51], indicating that GQD was successfully prepared in the experiment. Figure 1B presents the UV-visible absorption spectrum of GQD. It can be seen that the characteristic absorption peak of GQD appears at 246 nm.

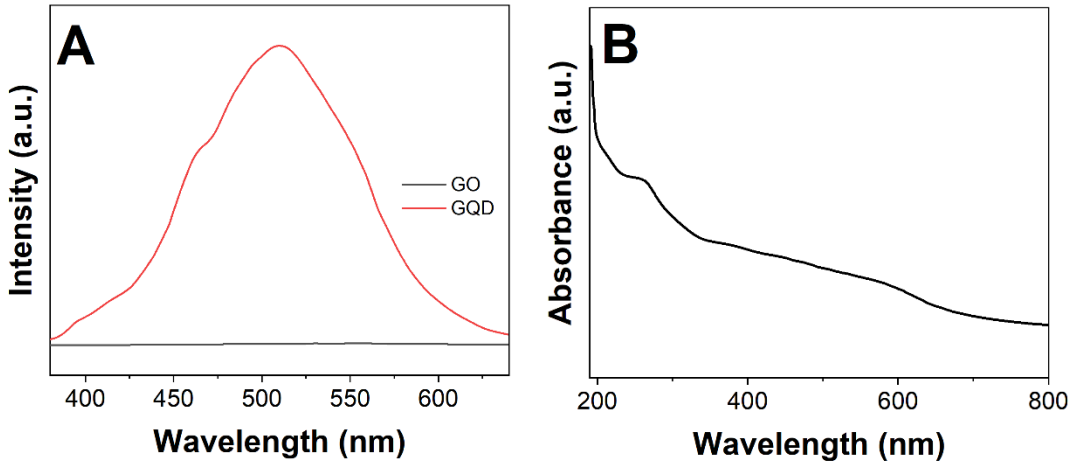

Figure 1. (A) PL spectra of GO and GQD dispersion. (B) UV-vis spectrum of GQD dispersion.

Figure 2 shows the SEM of Parg/GCE and GQD/Parg/GCE. As can be seen from the figure, when Parg was modified to the electrode surface, the electrode surface was covered with neatly arranged polymer films of polyarginine [52], whereas the morphology became slightly rough as GQD was further modified on the electrode surface. For the purpose of demonstrating that Parg polymerized on the electrode surface, arginine and Parg were analyzed with Fourier transform infrared spectroscopy (FTIR) in this study. It can be seen from the arginine infrared spectrum that 3367-3300 cm^{-1} absorption band is corresponding to NH, NH_2 and NH_3 groups of ν(N - H) vibration peak, and 2832-3009 cm^{-1} absorption band is caused by the ν(O - H) and ν(C - H) vibration peak overlap. The absorption peaks of C=N and C—N correspond to 1679 cm^{-1} and 1036 cm^{-1} [53], respectively. The absorption peaks of Parg at 1643 cm^{-1} correspond to stretching vibration peaks of C=O and C=N [54]. The peaks located at 1113 and 3298 cm^{-1} can be ascribed to the stretching vibrations of C —N and N—H [55–58], respectively.

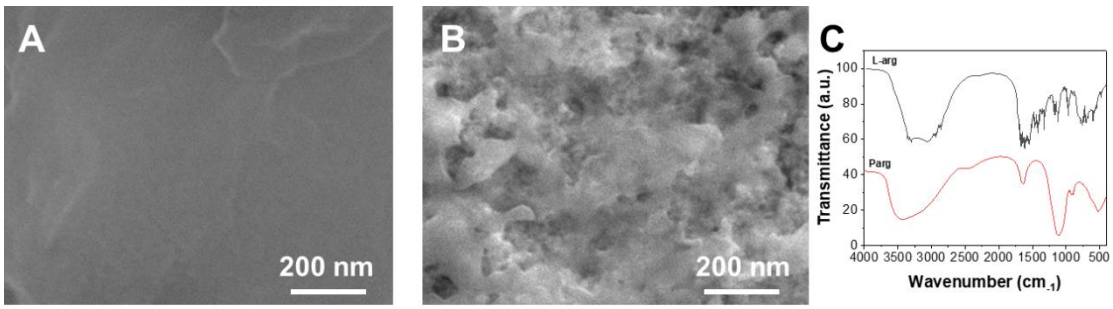

Figure 2. SEM image of (A) Parg/GCE and (B) GQD/Parg/GCE. (C) FTIR spectra of L-arg and Parg.

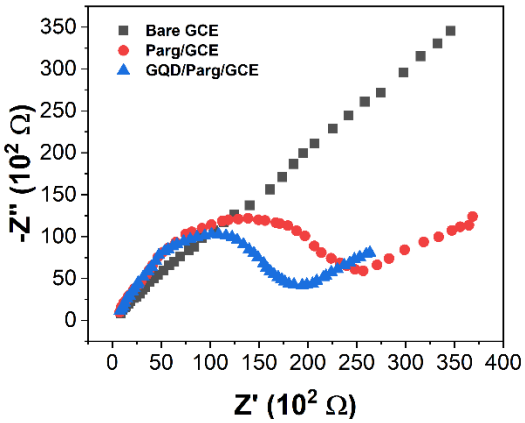

Figure 3. EIS spectra of bare GCE, Parg/GCE and GQD/Parg/GCE in 10 mM ($[Fe(CN)6]^{3-/4-}$).

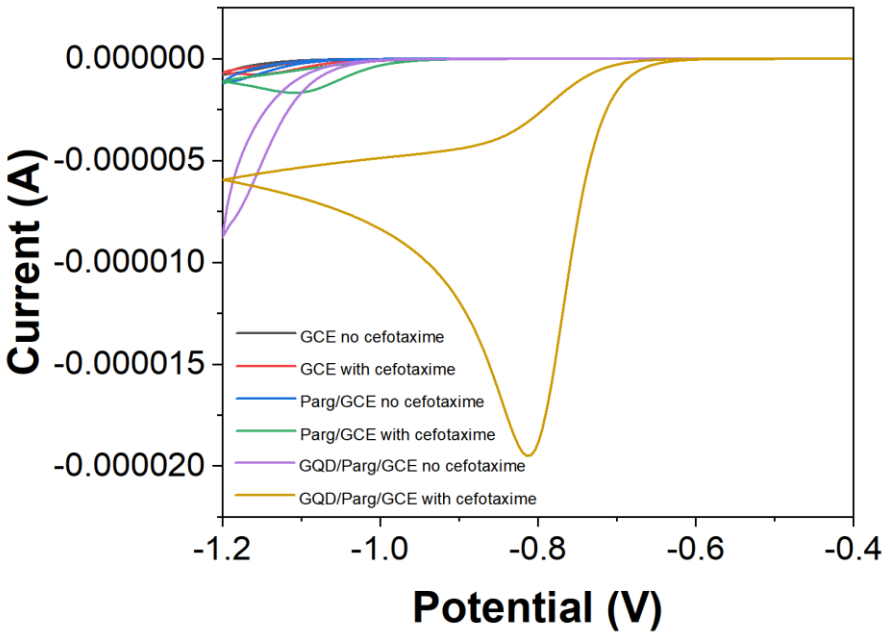

Figure 4. CV of GCE, Parg/GCE and GQD/Parg/GCE in the absence and presence of 0.1 mM cefotaxime (0.1 M B-R buffer, pH 4.5, scan rate: 50 mV/s).

The EIS can be adopted to study the change of the electrode interface impedance with the modification process through the observation of the steady-state reaction of the electrode/solution system to the small amplitude ac signal disturbance. As shown in Figure 3, the EIS of bare glassy carbon electrode basically presents a straight line, indicating that the electrode process is controlled by diffusion [59]. The EIS of Parg/GCE electrode appears arc-shaped in the high-frequency region, but linear in the low-frequency region, indicating that Parg film has a certain hindrance effect on electron transfer. The semi-arc of GQD/Parg/GCE is reduced, demonstrating that the introduction of GQD can improve the performance of the electrode.

Figure 4 reveals the CV diagrams of GCE, Parg/GCE and GQD/Parg/GCE with and without 0.1 mM cefotaxime. The results show that there are no obvious redox peaks in the buffer solution when the potential is between -0.3 V and -1.2 V [60]. However, irreversible reduction reaction of cefotaxime occurs on GCE with cefotaxime being added into buffer solution, and its reduction peak shape is wider and peak current is smaller, whereas on Parg/GCE, cefotaxime shows an obvious reduction peak, and the peak current increases. Compared with GCE, the reduction peak potential of Parg/GCE on the modified electrode shifts positively, and the peak current increases significantly, indicating that GQD has a good electrocatalytic reduction effect on cefotaxime [61]. On the other hand, GQD/Parg/GCE show better electrochemical catalytic performance.

Many different experimental parameters can be applied in an experimental system, and the change of experimental parameters exerts different effects on the experimental results. It can be confirmed that the concentration of arginine can affect the current response. Figure 5 shows the influence of arginine concentration changes on cefotaxime oxidation current. As presented in the figure, the oxidation current of cefotaxime gradually increases. However, when the concentration of L-arg is greater than 1 mM, the oxidation current of cefotaxime tends to decline, which indicates that excessively thick Parg film may hinder the conductivity of the film. Therefore, 1 mM was chosen to be the optimal polymerization concentration of arginine.

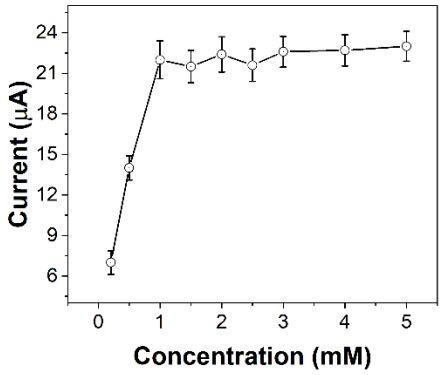

Figure 5. The effect of the concentration of L-arg during the electro-polymerization towards sensing performance.

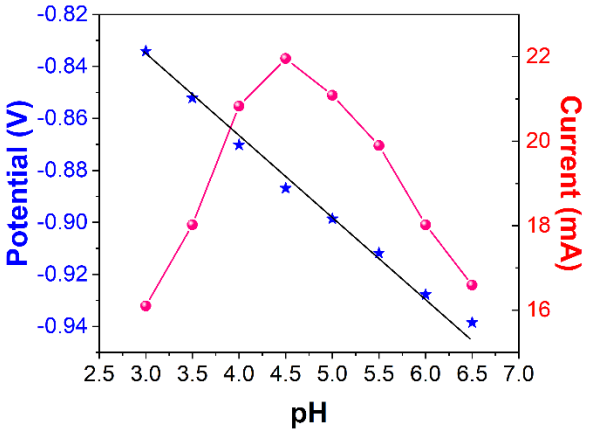

Figure 6. Relationship of Ep and Ip with pH (3.0, 3.5, 4.0, 4.5, 5.0, 5.5, 6.0, 6.5)recorded using CV scan (50 mV/s).

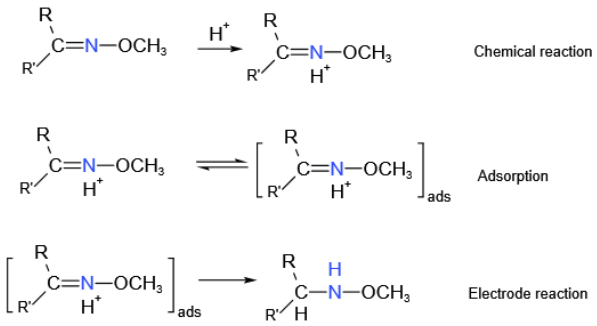

Figure 7. Mechanism of cefotaxime oxidation of the electrode surface.

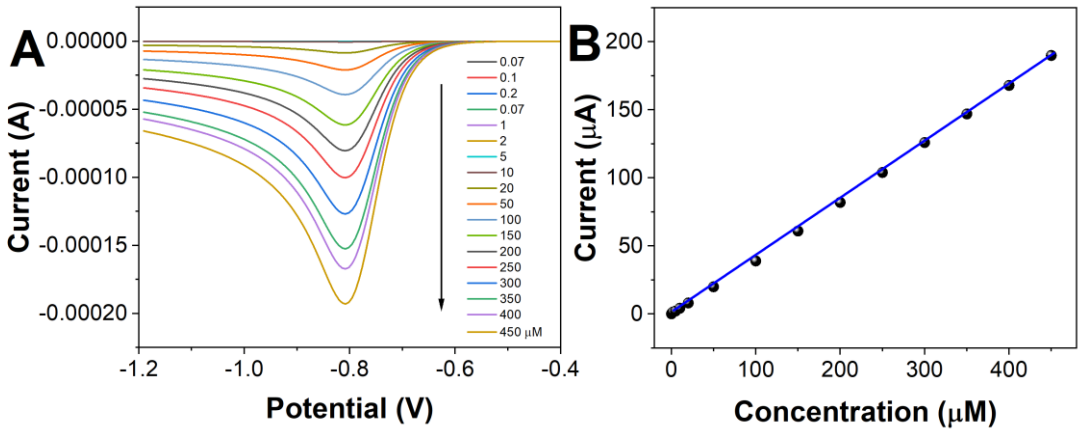

Figure 8. (A) DPV curves of GQD/Parg/GCE towards different concentrations of cefotaxime. (B) Plots of peak currents vs cefotaxime concentrations(0.1 M B-R buffer, pH 4.5, pulse amplitude: 50 mV; pulse width: 0.05 s; pulse period: 0.5 s).

Figure 6 shows CV measurement in buffers containing 0.1 mM cefotaxime at different pH values. As the pH value reaches 4.5, the reduction peak current is the maximum, thus the buffer solution pH =

4.5 is selected. The linear regression equation between Ep (V) and pH is as follows: Ep (V) = -0.0281ph-0.0749, r = 0.9989. The number of electrons involved in cefotaxime reduction is twice that of protons. Therefore, it can be inferred that the reaction of cefotaxime on the modified electrode is reaction of 2 electrons and 1 proton. Thus, it can be speculated that electrode reaction may occur on oxime bond, and its reaction mechanism is shown in Figure 7.

In the buffer system, GQD/Parg/GCE was adopted as the working electrode to determine the differential pulse voltammetry of cefotaxime solutions with different concentrations (Figure 8). There is a good linear relationship between GQD/Parg/GCE and Ip in the concentration range of 70 nM ~ 1 μM and 1 μM ~ 45 0 μM. The detection limit is 34· nM (S /N = 3).

After each measurement, the electrode was scanned by cyclic voltammetry in blank substrate to remove the adsorbed cefotaxime on the electrode surface, thus restoring its catalytic activity. Table 1 shows the comparison of the performance of our proposed sensor with other reported sensors.

Table 1. Linear range and LOD obtained using proposed electrochemical sensor and other electrochemical sensors reported for the cefotaxime sensing.

Sensor	Linear range	LOD	Reference
Au–PtNPs/MWCNT/GCE	0.004–10.0 μM	1 nM	[62]
Au-PDA@SiO_2/rGO/GCE	0.001–5 μM	0.01 nM	[63]
NaMM/ERGO/CPE	0.0005–2.4 μM	0.1 nM	[64]
FeNP/GCE	0.15–25 μM	100 nM	[65]
AuNPs/Parg/CPE	0.01–100 μM	2 nM	[66]
GQD/Parg/GCE	70 nM – 450 μM	34 nM	This work

The same modified electrode was adopted for 10 times of parallel determination of 15 μM cefotaxime, and the relative standard deviation (RSD) was 3.11%. The RSD of the parallel electrode was 2.67% after 8 measurements, which indicates that GQD/Parg/GCE has good repeatability and reproducibility. The modified electrode was adopted once a day and placed at room temperature, and the peak current only decreased by 4.22% after 10 days. 30 days later, the peak current remained 83.6% of the first measured current, demonstrating the good stability of the modified electrode.

Table 2. The detection results and recoveries of the cefotaxime tablets samples using proposed GQD/Parg/GCE.

Sample	Detected (μM)	Added (μM)	Found (μM)	Recovery (%)
Tablet 1	4.17	2.00	6.15	99.68
Tablet 2	4.20	5.00	9.13	99.24
Tablet 3	4.21	10.00	14.30	100.63

10 mg cefotaxime sodium injection powder produced by different manufacturers was weighed and dissolved in water to a constant volume of 100 mL. The solution was removed from 1 mL to 50 mL volumetric flask and the volume was fixed with a B-R buffer solution of pH = 4.5. A certain amount was taken in the electrolytic cell, and the content of cefotaxime was measured according to the above optimal experimental conditions. In addition, the standard recovery experiment was carried out, with the results shown in Table 2. The recoveries are 99.24% ~ 100.63%, which can meet the requirement of conventional analysis.

4. CONCLUSION

In this study, an electrochemical sensor was constructed based on GQD and was applied in the detection of the cefotaxime concentration. Parg can effectively improve the electrochemical response of the electrode to cefotaxime and reduce the overpotential effect of cefotaxime. The introduction of GQD can further increase the sensing performance. Electrochemical analysis of cefotaxime with GQD/Parg/GCE shows a wide linear range, as well as good stability and reproducibility. Due to the advantages of easy preparation, low cost and simple sample pretreatment, it is concluded that GQD/Parg/GCE can be applied to the analysis and detection of daily cefotaxime concentration in the near future.

References

1. X. Yue, Z. Li, S. Zhao, *Microchem. J.*, 159 (2020) 105440.
2. G. Moro, F. Bottari, N. Sleegers, A. Florea, T. Cowen, L.M. Moretto, S. Piletsky, K. De Wael, *Sens. Actuators B Chem.*, 297 (2019) 126786.
3. M. Wang, M. Hu, J. Liu, C. Guo, D. Peng, Q. Jia, L. He, Z. Zhang, M. Du, *Biosens. Bioelectron.*, 132 (2019) 8.
4. K. Rudnicki, K. Sipa, M. Brycht, P. Borgul, S. Skrzypek, L. Poltorak, *TrAC Trends Anal. Chem.*, 128 (2020) 115907.
5. Z. Li, C. Liu, V. Sarpong, Z. Gu, *Biosens. Bioelectron.*, 126 (2019) 632.
6. Q. Wang, Q. Xue, T. Chen, J. Li, Y. Liu, X. Shan, F. Liu, J. Jia, *Chin. Chem. Lett.*, 32 (2021) 609.
7. H. Karimi-Maleh, Y. Orooji, F. Karimi, M. Alizadeh, M. Baghayeri, J. Rouhi, S. Tajik, H. Beitollahi, S. Agarwal, V.K. Gupta, *Biosens. Bioelectron.* (2021) 113252.
8. M. Chen, H. Yang, Z. Song, Y. Gu, Y. Zheng, J. Zhu, A. Wang, L. Fu, *Phyton-Int. Exp. Bot.*, 90 (2021) 1507.
9. H. Shi, L. Fu, F. Chen, S. Zhao, G. Lai, *Environ. Res.*, 209 (2022) 112747.
10. H. Karimi-Maleh, A. Khataee, F. Karimi, M. Baghayeri, L. Fu, J. Rouhi, C. Karaman, O. Karaman, R. Boukherroub, *Chemosphere* (2021) 132928.
11. A.J. dos Santos, M.S. Kronka, G.V. Fortunato, M.R.V. Lanza, *Curr. Opin. Electrochem.*, 26 (2021) 100674.
12. A. Joshi, K.-H. Kim, *Biosens. Bioelectron.*, 153 (2020) 112046.
13. Z. Bitew, M. Amare, *Electrochem. Commun.*, 121 (2020) 106863.
14. N.S. Alsaiari, K.M.M. Katubi, F.M. Alzahrani, S.M. Siddeeg, M.A. Tahoon, *Micromachines*, 12 (2021) 308.
15. N. Sleegers, A.L. van Nuijs, M. van den Berg, K. De Wael, *Anal. Chem.*, 93 (2021) 2394.
16. R. Guo, X. Xu, Z. Sun, X. Hu, *Environ. Technol.*, 43 (2022) 893.

17. Y. Benrighi, N. Nasrallah, T. Chaabane, V. Sivasankar, A. Darchen, O. Baaloudj, *Opt. Mater.*, 115 (2021) 111035.
18. L. Fu, X. Zhang, S. Ding, F. Chen, Y. Lv, H. Zhang, S. Zhao, *Curr. Pharm. Anal.*, 18 (2022) 4.
19. L. Karadurmus, K. Eşme, N.K. Bakirhan, S.A. Ozkan, *Curr. Pharm. Anal.*, 16 (2020) 337.
20. Q. Wang, D. Wang, J. Wang, Y. Cui, H. Xu, *Int J Electrochem Sci*, 14 (2019) 8639.
21. Z. Zhou, Z. He, S. Yin, X. Xie, W. Yuan, *Compos. Part B Eng.*, 220 (2021) 108984.
22. S. Chen, Q. Chen, Q. Li, J. An, P. Sun, J. Ma, H. Gao, *Chem. Mater.*, 30 (2018) 1782.
23. A. Saenchoopa, W. Boonta, C. Talodthaisong, O. Srichaiyapol, R. Patramanon, S. Kulchat, *Spectrochim. Acta. A. Mol. Biomol. Spectrosc.*, 251 (2021) 119433.
24. R. Goodarzi, R. Yousefimashouf, I. Sedighi, A. Moradi, F. Nouri, M. Taheri, *J. Adv. Med. Biomed. Res.*, 30 (2022) 47.
25. S. Christoforidou, E. Karageorgou, M. Ioannidou, E. Psomas, M. Maggira, G. Samouris, *Czech J. Food Sci.*, 38 (2020) 63.
26. F.-D. Munteanu, A.M. Titoiu, J.-L. Marty, A. Vasilescu, *Sensors*, 18 (2018) 901.
27. H. Karimi-Maleh, F. Karimi, L. Fu, A.L. Sanati, M. Alizadeh, C. Karaman, Y. Orooji, *J. Hazard. Mater.*, 423 (2022) 127058.
28. S.S.J. Princy, J.J. Sherin, C. Vijayakumar, C. Hentry, M. Bindhu, K.M. Alarjani, N.S. Alghamidi, D.S. Hussein, *Environ. Res.*, 210 (2022) 112883.
29. R. Sukanya, K. Balamurugan, S.-M. Chen, R. Rajakumaran, K. Muthupandi, J.-J. Shim, C.B. Breslin, *Materials*, 14 (2021) 6700.
30. L. Eskandari, F. Andalib, A. Fakhri, M.K. Jabarabadi, B. Pham, V.K. Gupta, *Int. J. Biol. Macromol.*, 164 (2020) 4138.
31. Y. Guo, Y. Luo, M. Tang, M. Zhang, M. Yuan, S. Chen, Q. Tu, J. Wang, *Sens. Actuators B Chem.*, 344 (2021) 130191.
32. M. Baghayeri, B. Mahdavi, Z. Hosseinpor-Mohsen Abadi, S. Farhadi, *Appl. Organomet. Chem.*, 32 (2018) e4057.
33. M. AbdEl-Mongy, A.S. Othman, H.A. Elkhateeb, *Egypt. J. Microbiol.*, 53 (2018) 193.
34. H. Karimi-Maleh, M. Alizadeh, Y. Orooji, F. Karimi, M. Baghayeri, J. Rouhi, S. Tajik, H. Beitollahi, S. Agarwal, V.K. Gupta, S. Rajendran, S. Rostamnia, L. Fu, F. Saberi-Movahed, S. Malekmohammadi, *Ind. Eng. Chem. Res.*, 60 (2021) 816.
35. H. Karimi-Maleh, C. Karaman, O. Karaman, F. Karimi, Y. Vasseghian, L. Fu, M. Baghayeri, J. Rouhi, P. Senthil Kumar, P.-L. Show, S. Rajendran, A.L. Sanati, A. Mirabi, *J. Nanostructure Chem.* (2022) in-press.
36. G. Das, H.-S. Shin, A. Kumar, C.N. Vishnuprasad, J.K. Patra, *Saudi J. Biol. Sci.*, 28 (2021) 980.
37. S. Alibi, D. Crespo, J. Navas, *Antibiotics*, 10 (2021) 231.
38. A.R. Khezripour, D. Souri, H. Tavafi, M. Ghabooli, *Measurement*, 148 (2019) 106939.
39. A. Mathur, H.C. Nayak, S. Rajput, S. Roy, S. Nagabooshanam, S. Wadhwa, R. Kumar, *Chemosensors*, 9 (2021) 339.
40. C. Chaicham, T. Tuntulani, V. Promarak, B. Tomapatanaget, *Sens. Actuators B Chem.*, 282 (2019) 936.
41. H. Karimi-Maleh, H. Beitollahi, P.S. Kumar, S. Tajik, P.M. Jahani, F. Karimi, C. Karaman, Y. Vasseghian, M. Baghayeri, J. Rouhi, *Food Chem. Toxicol.* (2022) 112961.
42. H. Karimi-Maleh, A. Ayati, R. Davoodi, B. Tanhaei, F. Karimi, S. Malekmohammadi, Y. Orooji, L. Fu, M. Sillanpää, *J. Clean. Prod.*, 291 (2021) 125880.
43. H. Karimi-Maleh, A. Ayati, S. Ghanbari, Y. Orooji, B. Tanhaei, F. Karimi, M. Alizadeh, J. Rouhi, L. Fu, M. Sillanpää, *J. Mol. Liq.*, 329 (2021) 115062.
44. Y. Zhang, C. Wu, X. Zhou, X. Wu, Y. Yang, H. Wu, S. Guo, J. Zhang, *Nanoscale*, 5 (2013) 1816.
45. J. Ju, W. Chen, *Anal. Chem.*, 87 (2015) 1903–1910.
46. M. Ali, M. Bacchu, M. Daizy, C. Tarafder, M. Hossain, M. Rahman, M. Khan, *Anal. Chim. Acta*, 1121 (2020) 11.

47. G. Tigari, J. Manjunatha, *J. Anal. Test.*, 3 (2019) 331.
48. Z. Xu, M. Peng, Z. Zhang, H. Zeng, R. Shi, X. Ma, L. Wang, B. Liao, *Front. Chem.*, 9 (2021) 683.
49. C. Li, F. Sun, *Front. Chem.*, 9 (2021) 409.
50. Y. Wang, L. Chen, T. Xuan, J. Wang, X. Wang, *Front. Chem.*, 9 (2021) 569.
51. D. Sebastian, S. Soman, *Luminescence*, 36 (2021) 1743.
52. W. Ju, X. Zhen, L. Zheng, *Biochem. Eng. J.*, 160 (2020) 107635.
53. F. Mokhtari, M. Hasanzadeh, A. Mokhtarzadeh, N. Shadjou, *Med. J. Tabriz Univ. Med. Sci.*, 41 (2019) 85.
54. A. Fujimura, S. Yasui, K. Igawa, A. Ueda, K. Watanabe, T. Hanafusa, Y. Ichikawa, S. Yoshihashi, K. Tsuchida, A. Kamiya, *Cells*, 9 (2020) 2149.
55. D. Salah, F.S. Moghanm, M. Arshad, A.A. Alanazi, S. Latif, M.I. El-Gammal, E.M. Shimaa, S. Elsayed, *Diagnostics*, 11 (2021) 1196.
56. B. Fan, Q. Wang, W. Wu, Q. Zhou, D. Li, Z. Xu, L. Fu, J. Zhu, H. Karimi-Maleh, C.-T. Lin, *Biosensors*, 11 (2021) 155.
57. Y. Zheng, D. Wang, X. Li, Z. Wang, Q. Zhou, L. Fu, Y. Yin, D. Creech, *Biosensors*, 11 (2021) 403.
58. L. Fu, A. Yu, G. Lai, *Chemosensors*, 9 (2021) 282.
59. Y. Li, Y. Ma, E. Lichtfouse, J. Song, R. Gong, J. Zhang, S. Wang, L. Xiao, *J. Hazard. Mater.*, 421 (2022) 126718.
60. J. Lei, P. Duan, W. Liu, Z. Sun, X. Hu, *Chemosphere*, 250 (2020) 126163.
61. S.K. SHUKLA, S. TANWER, *J. Turk. Chem. Soc. Sect. Chem.*, 8 (2021) 1099.
62. S. Shahrokhian, S. Rastgar, *Analyst*, 137 (2012) 2706.
63. M.Z.H. Khan, M. Daizy, C. Tarafder, X. Liu, *Sci. Rep.*, 9 (2019) 19041.
64. S. Dehdashtian, M. Behbahani, A. Noghrehabadi, *J. Electroanal. Chem.*, 801 (2017) 450.
65. M. Wang, X. Xu, J. Yang, X. Yang, Z. Tong, *Micro Nano Lett.*, 6 (2011) 284.
66. F. Zhang, S. Gu, Y. Ding, L. Zhou, Z. Zhang, L. Li, *J. Electroanal. Chem.*, 698 (2013) 25.